



HAL
open science

Critical assessment of the metrics for the evaluation of wall energy efficiency in transient regime

Julien Berger, Jean-Henry Ferrasse, Suelen Gasparin, Olivier Le Métayer,
Benjamin Kadoch

► To cite this version:

Julien Berger, Jean-Henry Ferrasse, Suelen Gasparin, Olivier Le Métayer, Benjamin Kadoch. Critical assessment of the metrics for the evaluation of wall energy efficiency in transient regime. 2022. hal-03840080

HAL Id: hal-03840080

<https://hal.science/hal-03840080>

Preprint submitted on 4 Nov 2022

HAL is a multi-disciplinary open access archive for the deposit and dissemination of scientific research documents, whether they are published or not. The documents may come from teaching and research institutions in France or abroad, or from public or private research centers.

L'archive ouverte pluridisciplinaire **HAL**, est destinée au dépôt et à la diffusion de documents scientifiques de niveau recherche, publiés ou non, émanant des établissements d'enseignement et de recherche français ou étrangers, des laboratoires publics ou privés.

Critical assessment of the metrics for the evaluation of wall energy efficiency in transient regime

Julien Berger^{a*}, Jean-Henry Ferrasse^b

Suelen Gasparin^{c,d}, Olivier Le Metayer^e, Benjamin Kadoch^e

November 4, 2022

^a Laboratoire des Sciences de l'Ingénieur pour l'Environnement (LaSIE), UMR 7356 CNRS, La Rochelle Université, CNRS, 17000, La Rochelle, France

^b Aix Marseille Univ, CNRS, Centrale Marseille, M2P2, Marseille, France

^c CEREMA, French Ministry of Ecological Transition, BPE Research Team, F-44000 Nantes, France

^d Univ. Savoie Mont Blanc, UMR 5271 CNRS, LOCIE, 73000 Chambéry, France

^e Aix Marseille Univ, CNRS, IUSTI, Marseille, France

*corresponding author, e-mail address : julien.berger@univ-lr.fr

Abstract

Within the environmental context, designing energy efficient buildings is crucial. The reliability of the standard metrics used to design and qualify efficiency is first discussed. Then, a metric is proposed based on the evaluation of the exergy destruction rate. It enables to assess the exergy loss in dynamic and transient condition. The metric is computed with the temperature and vapor pressure obtained with a coupled heat and mass transfer model. The approach is tested with experimental data obtained from a wood fiber wall demonstrator. The proposed metrics allows a more accurate assessment, particularly in dynamic and transient conditions. Two periods are considered, one with negligible and one with mass transfer through the wall. The mass transfer can account for 30% in the exergy destruction. It is also demonstrated that during a "winter climate" a satisfying approximation of the metric can be obtained if heat transfer model is used alone as in building simulation programs.

Key words: Wall energy efficiency; Thermal conductance; Heat transfer coefficient; Entropy generation; Second law analysis; transient; steam transport

1 Introduction

The building construction is one of the most energy-consumer sectors in Europe with 28% of final energy consumption [1]. To face this issue and its environmental consequences, public policies have been and are being put in place. The European Union has developed a legislative framework [2] to stimulate the performance and energy efficiency of buildings and thus achieve a highly energy efficient and decarbonized building stock by 2050. The 2015 French law on the "Energy Transition for Green Growth" plans to increase the share of renewable energy by 32% in 2030 and to reduce energy consumption by 50% in 2050 compared to 2012 levels [3]. Thermal regulations [4] became more demanding in France in 2005 and 2012. The 2022 environmental regulation [5] takes into account, in addition to energy consumption, all the carbon emissions of a building from its construction phase to its dismantling.

One of the levers to reach these objectives is to improve the efficiency of the building envelope in a framework of renovation of old buildings and construction of zero emission ones. In addition control strategies for efficient heating and cooling should be adapted to avoid energy waste. It seems then obvious that time dependent metrics are required in the building industry to decrease energy consumption. To do this, it is necessary to define what a "good" wall is. Obviously, for winter configurations (when the outside temperature is lower than the inside one), an efficient wall must reduce at most the outward heat flux. Expectations are similar for

summer configurations (when the outside temperature is higher than the inside one) with the inward heat flux. The definition of a “good” wall becomes more complicated for intermediate configurations, *i.e.* when the outside temperature varies higher and lower than the inside one during the same day. Assuming for instance in spring a day with high incident radiation and a cold night. During the night, the outward heat transfer should be minimized. However, during the day, the inward flux should be maximized to provide *free* heating source to the inside energy balance and occupant thermal comfort. Thus, a metric to qualify the energy efficiency of a wall should unify such antagonistic periods.

Several metrics for qualifying an energy efficient wall have been proposed in the literature. A very common one is the thermal transmittance U (also referred as heat transfer coefficient). This metric has become a standard with the norm ISO 6946:2017 [6]. In France, it is defined by the 2005 and 2012 [7] thermal regulations. This metric plays an important role in the design of energy efficient buildings since it is an input of building energy simulation programs [8]. It is an average coefficient of the heat losses through the walls assuming a steady state transfer and a fixed in time temperature difference between inside and exterior zones. Among several works in the literature, this quantity has been used in [9] to predict the monthly heating demand for single-family residential sector in temperate climates. In recent works, inverse techniques have been employed in [10] and [11] to estimate such coefficients for building walls. An extension of its computation can be used for transient regimes to measure and monitor the time varying transmittance of a wall [12–14]. The use of this metric easy to calculate answers a very simple (and important) criterion. The more a wall is design to insulate the more it is efficient.

Another metric is used in the literature, denoted as the thermal loads of the wall. It is computed by integrating over time the heat flux on the inside surface. Numerous works are available in the literature using this metric. One can cite [15] or [16] where the authors evaluate the optimal thickness insulation based on the thermal loads to evaluate the energy cost. Note that this metric is an integrated one, *i.e.* often evaluated over a whole period (months or years). Thus, it is not designed for analysing and assessing on short time periods, the energy efficiency.

Despite their widely use, the two above-mentioned metrics do not consider correctly the thermal inertia in the assessment of the energy efficiency. In other words, the phase offset between the outside temperature and the instantaneous heat flux transmitted to the inside zone is not well integrated. Those metrics are based only on the first principles of thermodynamic, *i.e.* the energy conservation. They do not evaluate the *quality* of the energy transferred. In brief, a metric defined for transient and alternative situations of cooling and heating demands is required. A thermodynamic approach could be considered to unify the two antagonistic areas of “thermal design”: the increase of heat transfer and the thermal insulation problems.

Other metrics have been proposed in the literature based on the analysis of the exergy linking first and second principles of thermodynamics. Works on the analysis of human body energy dissipation can be mentioned. In [17], the human body is modeled by a lumped capacitance model to assess the temperature. In [18], a complete transient 3-dimensional heat transfer model is used. In [19], the body interaction with the building wall is taken into account. However, the latter is modeled in steady state and the exergy analysis focuses on the body. Works focusing on building walls can be highlighted. Particularly, STRUB and co-workers in [20] compares the wall to a thermodynamic engine. It can theoretically produce work by receiving heat from a hot source and rejecting it to the cold source. However, due to its underlying hypothesis, such metric cannot provide an instantaneous evaluation of the energy efficiently used but only time average value as the integration of the variation of ambient temperature should be equal to zero. The objective of this paper is twofold. First, a discussion of the reliability of the standard metrics in transient conditions for a real wall monitored during a heating configuration is given. Then, an alternative metric is proposed based on thermodynamic analysis according to first and second principles. Similar proposals for heat transfer have been done in the literature [21–23]. However, the case study are limited to constant in time [23] or periodic [21, 22] boundary

conditions. Here, real weather-based data are considered as boundary conditions. In addition, a coupled heat and mass model is used and compared with an heat transfer only model. The article is structured as follows. Section 2 applies the thermodynamic principles to the wall to propose an energy efficiency metric. Two approaches are considered. The first one assumes only heat transfer as most of the building simulation programs used for standard designs [24]. The second approach models coupled heat and mass transfer in the wall considered as an homogeneous porous materials. In Section 3, all the metrics are evaluated and compared for a real case study based on an experimental demonstrator of a wood fiber wall monitored during 14 days. Last, some conclusions and outlooks are proposed in Section 4.

2 Thermodynamic analysis

2.1 System under investigations

The system under consideration is the wall. A schematic representation of the enclosure is presented in Figure 1. The domain is defined by $x \in \Omega_x$ where $\Omega_x = [0, \ell]$ and ℓ [m] is the total wall length. The investigations are carried for the time interval $t \in \Omega_t = [0, t_f]$, where t_f [s] is the horizon of investigations. On the inside part, the temperature and relative humidity are controlled by HVAC systems. On the exterior part, the wall is exposed to dynamic climatic conditions. Heat and mass flow rates occur at the interfaces $x = 0$ and $x = \ell$. As a consequence, both the temperature $T(x, t)$ [K] and vapor pressure $P_v(x, t)$ [Pa] vary according to space and time in the wall.

Only winter configuration is considered for this study. Thus, the inside temperature T_{ins} is always considered higher to the exterior one T_{ext} during the whole time interval

$$T_{\text{ins}}(t) > T_{\text{ext}}(t), \quad \forall t \in \Omega_t, \quad (1)$$

so that heat losses are directed to the exterior. The direction of the mass flow rate may fluctuates. The HVAC systems which maintain constant the internal temperature and the relative humidity are not part of the investigated system.

In the following sections, the thermodynamic principles are first recalled. Two cases are considered to calculate the heat exchanged: without and with mass transfer inside the wall. It will be shown than the first thermodynamic principle can be calculated only by the knowledge of the temperature and steam pressure distribution in the wall.

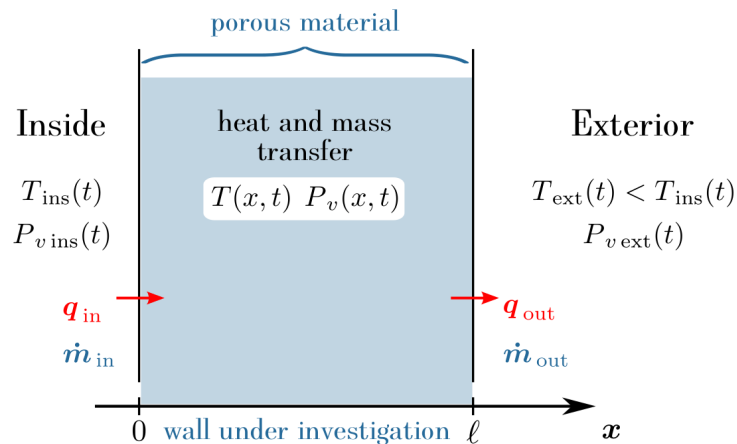


Figure 1. Illustration of the physical problem of heat and mass transfer.

2.2 First principle – applied only to heat transfer

The first principle is used in transient regime for the system exchanging heat with the inside (the building) and the ambient (the exterior of the building), the work transfer rate (mechanical, electrical, magnetic, ...) is assumed null in this system:

$$\frac{dE}{dt} = q_{\text{in}} - q_{\text{out}}, \quad (2)$$

where E [J] is the total energy of the system, computed according to:

$$E - E_0 = \int_0^\ell \int_{T_0}^T \rho c A d\mathcal{T} dx, \quad (3)$$

where ρ [$\text{kg} \cdot \text{m}^{-3}$], c [$\text{J} \cdot \text{kg}^{-1} \cdot \text{K}^{-1}$] and A [m^2] are the dry density, the heat capacity of the material and the surface area of the wall, respectively. The temperature T_0 is the arbitrary reference temperature for a reference energy E_0 . The quantities q_{in} [W] and q_{out} [W] are the inward and outward heat transfer rate through the system, respectively, with the inside at temperature T_{ins} and ambient with T_{ext} . In this particular configuration, characterized by Eq. (1), the heat transfer rate with ambient coincides with heat losses as illustrated in Figure 2.

To evaluate heat rates, they are computed considering conductive heat transfer in the wall by:

$$q_{\text{in}} = -k A \left. \frac{\partial T}{\partial x} \right|_{x=0}, \quad q_{\text{out}} = -k A \left. \frac{\partial T}{\partial x} \right|_{x=\ell}, \quad (4)$$

where k [$\text{W} \cdot \text{m}^{-1} \cdot \text{K}^{-1}$] is the thermal conductivity. Thus, the calculation of the three terms in the first principle requires only the knowledge of the temperature T inside the wall. The temperature is computed by solving the heat diffusion equation for $(x, t) \in \Omega_x \times \Omega_t$ as presented in [25].

The temperature in the wall is computed using a numerical model with a non-conservative numerical scheme. Thus, unavoidable numerical approximations are introduced that can be evaluated through the error on the first principle balance Eq. (2) with the following quantity:

$$\Delta = \frac{1}{q_{\text{in}}} \left(\frac{dE}{dt} + q_{\text{out}} \right) \quad (5)$$

If the first principle is verified (*i.e.* no numerical errors at all), then $\Delta = 1$. The difference between Δ and unity provides an indication of the accuracy of the numerical method of the model.

2.3 First principle – applied to coupled heat & mass transfer

Here, both heat and mass transfer are taken into account in the wall model. For the thermodynamic analysis and for the sake of clarity with Section 2.2, a different letter typography is used for the quantities. The inward and outward heat flow rate are now computed by considering the enthalpy of the flow. A "lumped" heat flow rate is used rather than an enthalpic flow and the heat transfer rate. As it will be seen, this will be of particular importance for comparison of metrics :

$$\mathfrak{q}_{\text{in}} = q_{\text{in}} + \dot{m}_{\text{in}} h^\circ, \quad \mathfrak{q}_{\text{out}} = q_{\text{out}} + \dot{m}_{\text{out}} h^\circ, \quad (6)$$

where $h^\circ = 2.5 \cdot 10^6 \text{ J} \cdot \text{kg}^{-1}$ is the latent heat of vaporization and the inward q_{in} and outward q_{out} heat flow rates are computed using Eq. (4). The latent heat of vaporization vary with temperature. However, as demonstrated in [26], a constant value still provides an accurate

approximation of the fields in the wall. Thus the first thermodynamic principle for the same system (assuming $\dot{W} = 0$) remains:

$$\frac{dE}{dt} = \mathbf{q}_{\text{in}} - \mathbf{q}_{\text{out}}, \quad (7)$$

where the internal energy is evaluated considering both the dry material and the water part:

$$E - E_0 = \int_0^\ell \int_{T_0}^T (\rho c + w(\phi) \cdot c_s) A dT dx, \quad (8)$$

where $c_s = 4180 \text{ J} \cdot \text{kg}^{-1} \cdot \text{K}^{-1}$ is the specific heat of liquid water and $w [\text{kg} \cdot \text{m}^{-3}]$ is the water content in the material, given by the adsorption curve. It is highlighted that w is a function of time and space since it depends on the relative humidity $\phi [-]$. The inward and outward mass flow rate through the system are denoted by $\dot{m}_{\text{in}} [\text{kg} \cdot \text{s}^{-1} \cdot \text{m}^{-2}]$ and $\dot{m}_{\text{out}} [\text{kg} \cdot \text{s}^{-1} \cdot \text{m}^{-2}]$, respectively. The latter are evaluated by:

$$\dot{m}_{\text{in}} = -\delta A \left. \frac{\partial P_v}{\partial x} \right|_{x=0}, \quad \dot{m}_{\text{out}} = -\delta A \left. \frac{\partial P_v}{\partial x} \right|_{x=\ell}, \quad (9)$$

where $\delta [\text{s}]$ is the vapor permeability of the material. Here, the temperature and vapor pressure inside the wall are computed by solving the heat and mass transfer equations detailed in [27].

Again the defined quantity $\Delta = 1$ will be used to evaluate the quality of the first principle.

2.4 Second principle and proposal of a metric

The second principle is now applied to the system. Note that, for the sake of compactness and without loss of generality, the developments are written using the typology of the coupled heat and mass transfer case. Writing the second principle in transient regime and for the defined system is equal to write the total entropy change $S_{\text{sys}} [\text{J} \cdot \text{K}^{-1}]$ at any times by:

$$\frac{dS_{\text{sys}}}{dt} = \left(\frac{dS_{\text{irr}}}{dt} + \frac{dS_{\text{exc}}}{dt} \right), \quad (10)$$

where S_{irr} and S_{exc} are the entropy due to irreversibility and to heat exchange respectively. Applied to the wall, Eq. (10) becomes:

$$\frac{dS_{\text{sys}}}{dt} = \left(\frac{dS_{\text{irr}}}{dt} + \frac{\mathbf{q}_{\text{in}}}{T_{\text{ins}}} - \frac{\mathbf{q}_{\text{out}}}{T_{\text{ext}}} \right). \quad (11)$$

A classical operation on both balances leading to exergy balance is obtained by subtracting to Eq. (7) (or Eq. (2), respectively), Eq. (11) multiplied by ambient temperature T_{ext} :

$$\frac{dE}{dt} - T_{\text{ext}} \cdot \frac{dS_{\text{sys}}}{dt} = \left(1 - \frac{T_{\text{ext}}}{T_{\text{ins}}} \right) \cdot \mathbf{q}_{\text{in}} - \frac{dS_{\text{irr}}}{dt} \cdot T_{\text{ext}}. \quad (12)$$

From Eq. (12), it is possible to isolate the destruction exergy Φ_d rate:

$$\dot{\Phi}_d = \frac{dS_{\text{irr}}}{dt} \cdot T_{\text{ext}} = - \left(\frac{dE}{dt} - T_{\text{ext}} \cdot \frac{dS_{\text{sys}}}{dt} \right) + \left(1 - \frac{T_{\text{ext}}}{T_{\text{ins}}} \right) \cdot \mathbf{q}_{\text{in}}. \quad (13)$$

The question of using a fluctuating ambient temperature has been abundantly discussed in literature. The discussion becomes crucial when the comparison with a reversible process is required. In the studied systems, this time dependent variable is of great importance as it makes vanish the exergy associated to the heat exchange with the ambient.

BEJAN [28] was the first to consider the wall as an engine and STRUB and co-workers in [20] used this idea to calculate the destruction of available work for a wall subjected to periodic heat

conditions. If the wall is considered as a system receiving heat from a hot source and rejecting heat to the ambient, it would be possible to produce work as stated by the CARNOT principle. As already mentioned, the work produced by the wall is assumed null. If the analogy with GOUY–STODOLA theorem [29] is kept, it coincides with the destruction of exergy rate in this system. That is why the destruction exergy rate quantity and its integration over time (exergy loss or destroyed exergy) as metrics of the energy efficiencies calculated by Eq. (14a) and (14b) will be used for the analysis:

$$\dot{\Phi}_d = \frac{\partial \Phi_d}{\partial t} = \frac{dS_{\text{irr}}}{dt} \cdot T_{\text{ext}}, \quad (14a)$$

$$\Phi_d = \int_0^{t_f} \dot{\Phi}_d dt. \quad (14b)$$

The integrated value over a defined period will be used to compare the behavior of the wall with metric from literature [20]. Eq. (14a) is computed using Eq. (13), knowing the distribution of the fields in the wall. The heat flow rate q_{ins} is evaluated according to Eq. (6). The entropy of the system S_{sys} is given by:

$$S_{\text{sys}} - S_0 = \int_0^\ell \int_{T_0}^T (\rho c + w(\phi) c_s) \frac{1}{T} d\mathcal{T} dx. \quad (15)$$

Then, the entropy rate is approximated by finite-differences method:

$$\frac{dS_{\text{sys}}}{dt} \approx \frac{S_{\text{sys}}(t + \epsilon) - S_{\text{sys}}(t - \epsilon)}{2\epsilon}, \quad \epsilon \rightarrow 0. \quad (16)$$

In [21–23], the authors proposed a numerical methods to directly compute these quantities. Here, the computation is carried *a posteriori*. The temperature and vapor pressure fields are first compute with the numerical models. Then, the integration and derivation operations are carried with numerical approximations.

The metric (14a) and (14b) are always positive since the rate of entropy due to irreversibility is always positive. It is composed of three terms, given by the right hand side of Eq. (13). The first two terms corresponds to the exergy rate of the wall and the last one to the exergy of exchanged heat. In winter configuration (Eq. (1)), the term $\left(1 - \frac{T_{\text{ext}}}{T_{\text{ins}}}\right)$ and the inward heat flow rate are both positive. To evaluate the effect of the exergy due to the heat transfer separately the quantity $\left(1 - \frac{T_{\text{ext}}}{T_{\text{ins}}}\right) \cdot q_{\text{in}}$ can also be plotted as a function of time. Once integrated in time this becomes the lost work mentioned in the literature part. That is why this quantity will be called lost work rate and written as \dot{W}_{lost} .

2.5 Calculation of metrics from the literature

Having proposed a metric for the evaluation of the energy efficiency of the wall, the metrics proposed in the literature are recalled. Usually in building design, the thermal transmittance U [$\text{W} \cdot \text{K}^{-1}$] is used to assess the wall energy efficiency. The original approach assumes a steady state heat transfer in the wall [30, 31] and proposes the following computation for a mono-layer wall:

$$U = \left(\frac{1}{h_{\text{ins}}} + \frac{\ell}{k} + \frac{1}{h_{\text{ext}}} \right)^{-1} A, \quad (17)$$

where h_{ins} [$\text{W} \cdot \text{m}^{-2} \cdot \text{K}^{-1}$] and h_{ext} are the inside and outside surface transfer coefficient. However, the metric Eq. (17) can be extended to a transient regime with the following formula [12]:

$$\tilde{U} = \frac{q_{\text{in}}}{T_{\text{ins}} - T_{\text{ext}}}. \quad (18)$$

Note that here, \tilde{U} is a function of time as the heat flow rate and as the temperatures are time dependant. The second metric is the thermal loads Q [J] metric, also widely used [15]:

$$Q = \int_0^{t_f} q_{\text{in}} dt. \quad (19)$$

It computes the total heat in terms of energy associated with the inward heat flow rate that went through the wall. This value is not cumulative as during summer heat flow is reverse compare to winter and then could come to be null or negative.

To cope with the fluctuating reference state, STRUB and co-workers in [20], proposed to calculate a metric for a long term evaluation to consider only the lost work resulting from the integration of the heat flow. It assumes that over a life time (typically one year for building energy efficiency), the fluctuation for energy and entropy in Eq. (13) vanishes. With such hypothesis, only the last term in Eq. (13) remains and the lost available work proposed in [20] is

$$\tilde{W}_{\text{lost}} \approx \int_0^{t_f} \left(1 - \frac{T_{\text{ext}}}{T_{\text{ins}}} \right) \cdot q_{\text{in}} dt. \quad (20)$$

It is important to remark that the three metrics Eqs. (18), (19), (20) are defined for only heat transfer in the literature and integrated on a period. However, for comparison with the proposed metrics, they will be extended for coupled heat and mass transfer thanks to the lumped heat transfer rate calculated in Eqs. (6).

3 Case study

3.1 Description

A schematic representation of the enclosure is presented in Figure 2(a). It is composed of two wood fiber layers of 8 cm each and one coating layer of 2 cm. This work only focuses on the wood fiber parts, so that the domain $\ell = 16$ cm corresponds to the total length of the two fiber layers. The experimental demonstrator of the enclosure has been built as presented in Figure 2(b) with more details in [26, 27, 32]. Several sensor have been placed to monitor the temperature T [K] and relative humidity ϕ [-]. Among all the sensors, only four are used in these investigations: two placed in the inside and exterior ambient air and two placed at $x = 0$ and $x = \ell$. Note that in the original works, three additional sensors are located inside the wood fiber layers. The monitoring have been carried out for 14 days. For the sake of clarity, the measured data are denoted with the super script $\hat{\cdot}$.

The smoothed measured temperature and vapor pressure on the inside and exterior parts are presented in Figures 3(a) and 3(b). The fields in the inside zone are well controlled by the HVAC systems. The vapor pressure is set around 1200 Pa before increasing to 2200 Pa after day 8. The temperature is set at 25 °C during the whole period. Regarding the exterior boundary conditions, the fields have daily oscillations due to climatic variations. The vapor pressure varies in the range of 1000 Pa, while the temperature varies between 5 and 20 °C. It can be remarked that the wall faces a winter configuration during the 14 days, *i.e.* the energy losses are directed outward. Three periods are selected for the thermodynamic analysis as illustrated in Figures 3(a) and 3(b). This choice is justified to select the transient part due to the increase of vapor pressure at day 8 independently of the two periods in interior stationary condition. The three time intervals are:

$$\Omega_t^1 = [0, 6] \text{ d.} \quad \& \quad \Omega_t^2 = [8, 14] \text{ d.} \quad \& \quad \Omega_t^3 = [6, 8] \text{ d.}$$

for the first, second and third period, respectively. The average exterior temperature is 11.9 °C, 10.6 °C and 9.5 °C for the first, second and third period, respectively.

Regarding the modeling, DIRICHLET boundary conditions are assumed prescribed by the measurement of temperature \hat{T} and vapor pressure \hat{P}_v at $x = 0$ and $x = \ell$. The initial condition is given by a fourth order polynomial using the measurements obtained by all sensors at $t = 0$. A coupled system of two nonlinear parabolic partial differential equations needs to be solved for the coupled heat and mass model:

$$c_M(T, P_v) \frac{\partial P_v}{\partial t} = \frac{\partial}{\partial x} \left(k_M(T, P_v) \frac{\partial P_v}{\partial x} \right),$$

$$c_T(T, P_v) \frac{\partial T}{\partial t} + c_{TM}(T, P_v) \frac{\partial P_v}{\partial t} = \frac{\partial}{\partial x} \left(k_T(T, P_v) \frac{\partial T}{\partial x} + k_{TM}(T, P_v) \frac{\partial P_v}{\partial x} \right),$$

where k_M and k_{TM} are total moisture transfer coefficients under vapor pressure gradient, k_T is the heat transfer coefficient under temperature gradient, c_M is the moisture storage coefficient, c_T is the energy storage coefficient and c_{TM} is the coupling storage coefficient. Details on these coefficients, boundary and initial conditions or numerical methods can be consulted in [27]. For the only heat transfer model, the governing equation is the classical diffusion one:

$$c_T \frac{\partial T}{\partial t} = \frac{\partial}{\partial x} \left(k_T \frac{\partial T}{\partial x} \right).$$

Both models are solved with a combined implicit–explicit approach numerical scheme based on centered finite-differences method. More details can be found in [27].

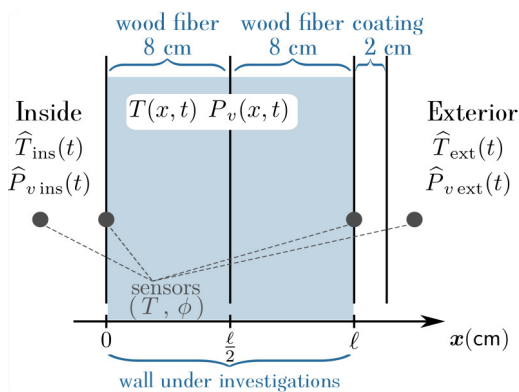
The material properties are the following: the density and specific heat of the material are $\rho = 146 \text{ kg} \cdot \text{m}^{-3}$ and $c = 1103 \text{ J} \cdot \text{kg}^{-1} \cdot \text{K}^{-1}$, respectively. The sorption curve is given by:

$$w = 7.063 \cdot 10^{-5} \phi^3 - 7.36 \cdot 10^{-3} \phi^2 + 0.4105 \phi + 0.2688 \text{ [kg} \cdot \text{m}^{-3}\text{]}.$$

For the coupled heat and mass transfer model, the thermal conductivity k and vapor permeability δ are depending on the water content and the relative humidity, respectively:

$$k = 6.97 \cdot 10^{-2} + 1.92 \cdot 10^{-4} w \text{ [W} \cdot \text{m}^{-1} \cdot \text{K}^{-1}\text{]}, \quad \delta = 3.28 \cdot 10^{-11} + 4.85 \cdot 10^{-12} \phi \text{ [s]}.$$

Note that for the only heat transfer model, the material properties at dry state ($\phi = w = 0$) are considered.



(a)



(b)

Figure 2. Illustration of the studied enclosure (a) and picture of the experimental demonstrator (b).

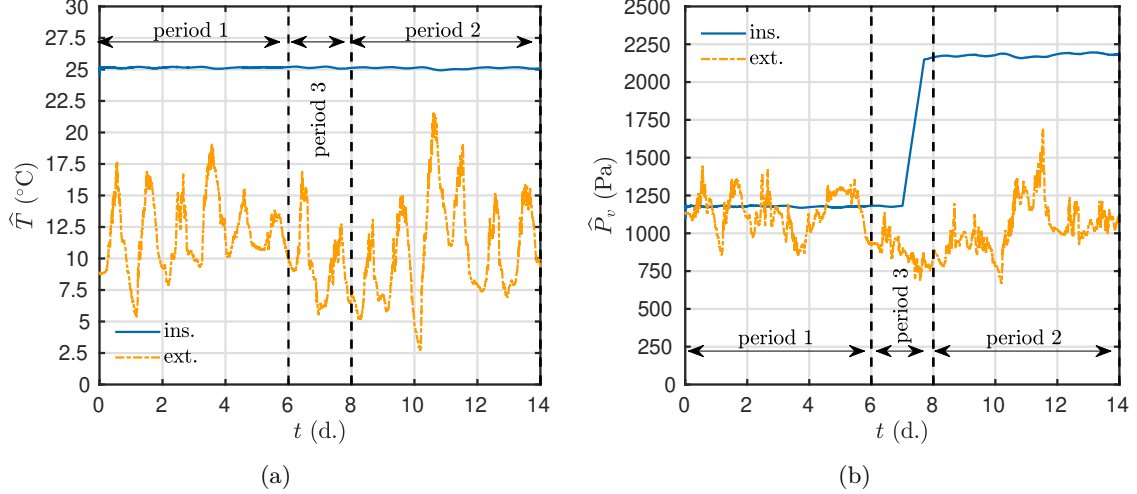


Figure 3. Time variation of the measured temperature (a) and vapor pressure (b) on the inside and outside parts of the wall.

3.2 Verification of the first principle

First, the results are analyzed regarding the first principle of thermodynamics. For the first period Ω_t^1 , figure 4(a) presents the time variation of the temperature computed with the coupled heat and mass transfer model. The variation follows the weather with a maximum for $T(x = \ell, t)$ around noon each day. As mentioned previously, the wall faces a winter configuration. Thus, the gradient of temperature in the wall is negative and the inward flux is always positive with smooth variations, as shown in Figure 4(b). The outward flux is almost always positive and more noisy. Occasionally, it becomes negative, corresponding to highest value of the outside temperature. In Figure 4(b), it can be noted that the heat flow rate due to the mass flow (latent effects) represents approximately $1 \text{ W} \cdot \text{m}^{-2}$ ($\sim 5 \%$) and $0.2 \text{ W} \cdot \text{m}^{-2}$ ($\sim 2 \%$) of the total outward and inward heat flow rate, respectively. Figure 4(c) displays the time variation of the internal energy rate and the Δ criteria defined by Eq. (5). The latter is equal to 1 over the whole period indicating that the first principle is verified by both models. Some small discrepancies, scaling with 5 %, can be remarked corresponding to the time when the outward flux is turbulent. These discrepancies are linked to the accuracy of the numerical scheme used to solve the governing equations of both models. Figure 4(d) presents the variation of the cumulative energy. The variation oscillates according to the climate weather data. The total variation vanishes with an approximate frequency of 24 h. Small differences are observed between the energy evaluated by the two models (at most $\sim 12 \%$). It is due to a low pressure gradient during the first period between the inside and outside parts of the wall as noted in Figure 3(b). Thus, the mass transfer is very small and the latent heat transfer almost negligible compared to the sensible one.

The results for the second period Ω_t^2 are given in Figure 5. Similar observations are found for the temperature variation. However, the latent heat transfer is more important for this period, as remarked in Figure 5(b). It corresponds to more than 10 % of the total for both inward and outward flows. This is due to an increase of the mass flow through the wall due to a higher vapor pressure gradient between inside and outside part (Figure 3(b)). Figure 5(c) shows that the first principle is well respected with a criteria Δ remaining around unity. Figure 5(d) presents the variation of the cumulative energy. Since the mass flow rate is more important for this second period, the differences in the internal energy between both models are higher (at most $\sim 30 \%$).

A very similar analysis can be carried for the third period Ω_t^3 in Figure 6. By verifying the first principle of thermodynamic for both models, it ensures that the temperature and vapor

pressure are computed accurately. Thus, other thermodynamic quantities such as heat flow, internal energy and entropy can be evaluated. Note that the time and space discretisation used in the numerical models have significant impact on the calculation of those quantities. Indeed, time and space integrations or derivations are needed to evaluate Eqs. (3), (8), (14b), (15) and (16). These computations are carried out with numerical approaches. The numerical convergence of the scheme is important. A particular attention is required on the numerical derivation (Eq. (16)) that tends to increase the numerical discretisation errors.

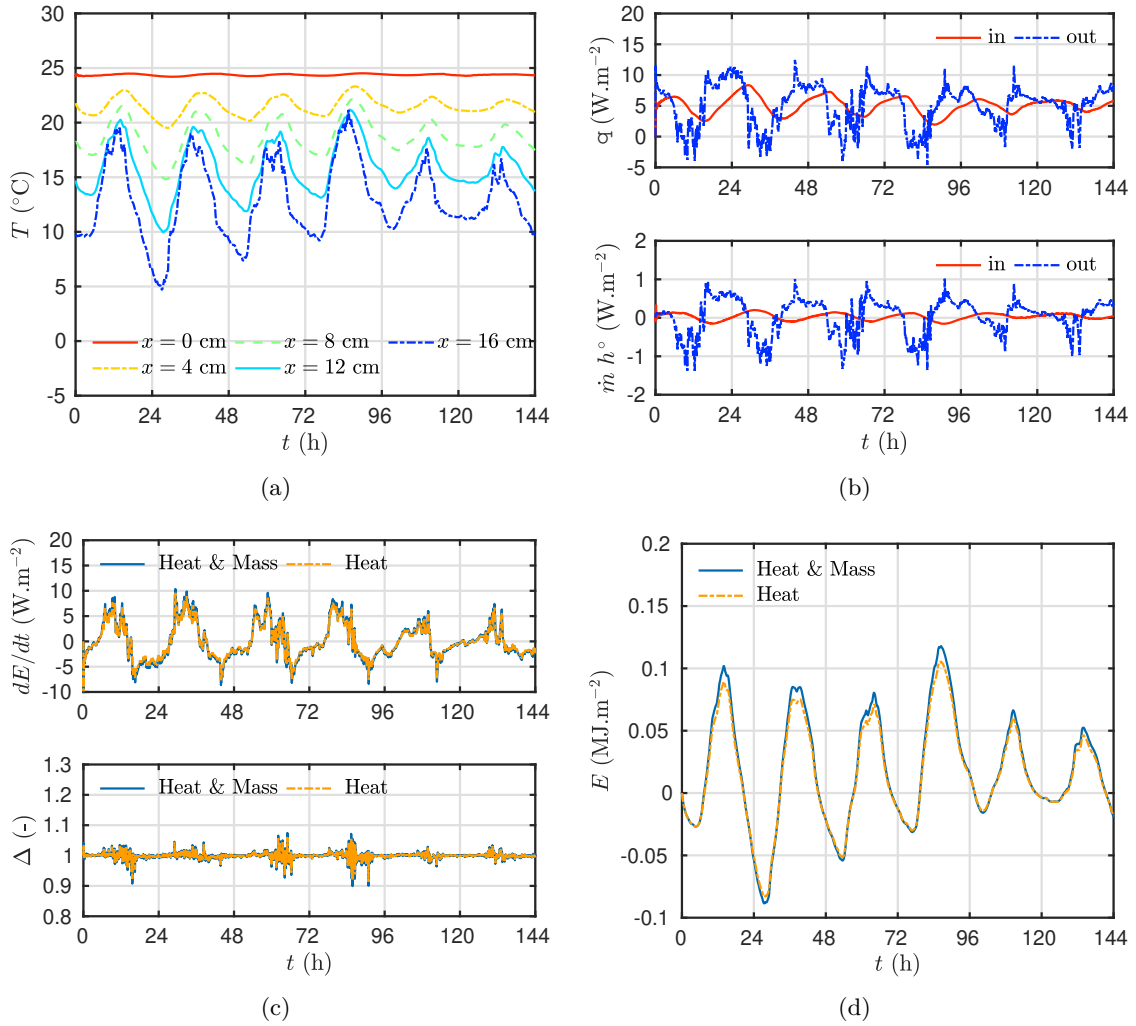


Figure 4. For the first period Ω_t^1 : time variation of computed temperature (a), heat flow rates (b), internal energy rate with Δ criteria (c) and cumulative internal energy (d).

3.3 Results

3.3.1 Exergy loss

Figures 7(a) to 7(d) present the exergy destruction of the wall for the three periods. Values integrated on the whole period are also presented in Tables 1 and 2. As expected, the cumulative exergy loss is positive and increasing since it corresponds to the entropy rate due to irreversibility. The small sinusoidal variations are due to the ones of the inward heat flow rate (see Figures 4(b) and 5(b)). With the heat transfer model, differences between the periods 1 and 2 can be related to the average outside temperature slightly lower. With the heat and mass model, due to higher heat flow rate induced by the increase of the latent effects, the exergy lost is increased for

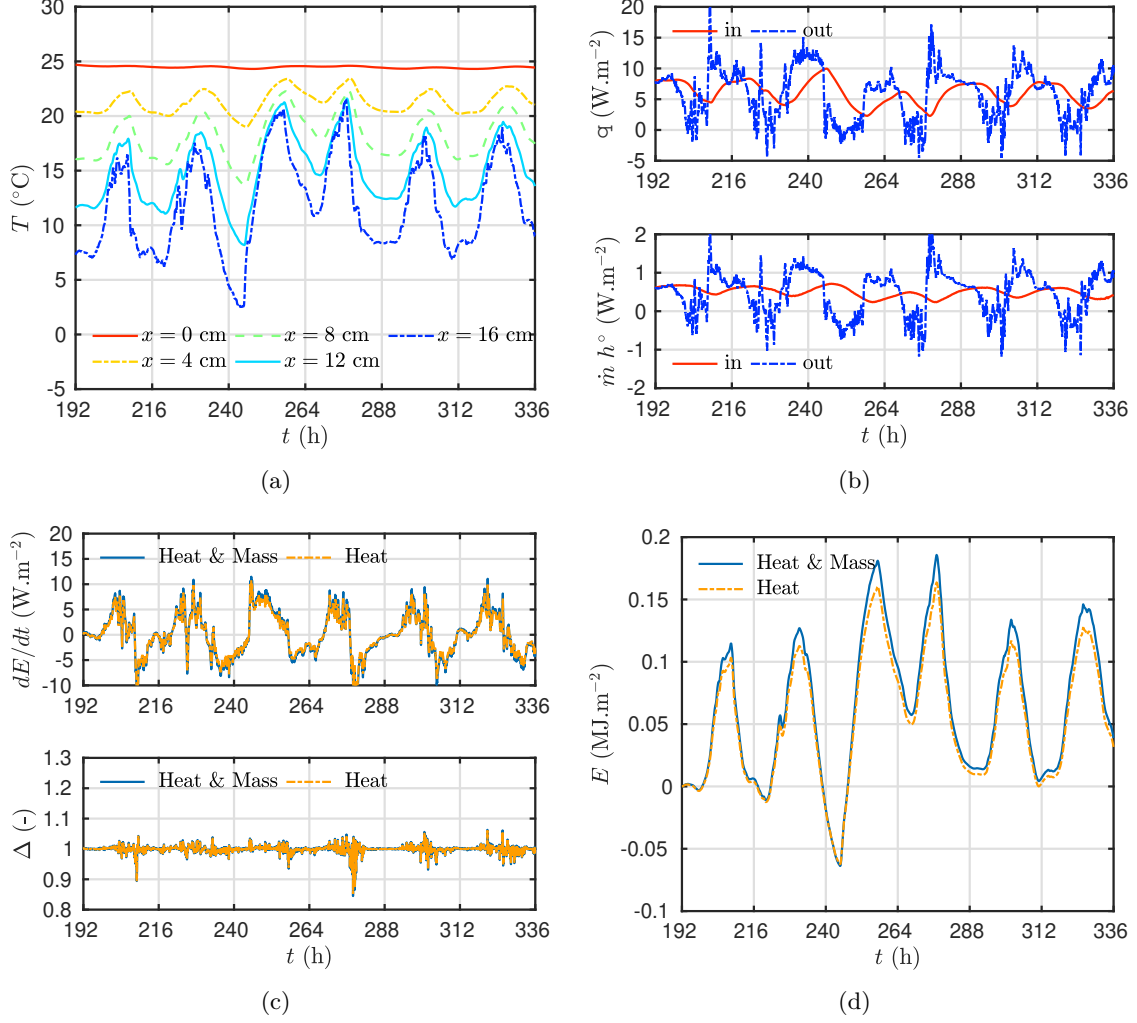


Figure 5. For the second period Ω_t^2 : time variation of computed temperature (a), heat flow rates (b), internal energy rate with Δ criteria (c) and cumulative internal energy (d).

the second period compared to the first one confirming the importance to take into account steam transport. During the first period where no transport occurs, the difference between both model is very small (123.4 and 125.0) confirming the role of steam. However, it is important to highlight that the heat transfer model enables a good first-order approximation of the loss of exergy. During the transient period it is very interesting to note that the value of exergy lost by day is almost 50% higher than during periods Ω_t^1 and 10% during Ω_t^2 confirming that transient process have a strong impact on exergy destruction. It appears that the proposed metric enables a precise analysis of the energy efficiency over time.

3.3.2 Comparison with metrics from literature

Figures 7(c), 7(d) and 8(b) compares the exergy destruction rate to the work rate and to standard metric U evaluated with Eq. (18). It highlights important discrepancies between metrics.

The variations have a phase shift, *i.e.* the minima and maxima do not occur at the same time instants. For instance, at $t \in \{12, 36, 84, 228, 252, 276\}$ h, the metric \tilde{U} is high indicating that an important heating is required in the inside zone to compensate the energy losses through the wall. At the same moment, the work rate \dot{W}_{lost} and the exergy destruction rate are both low.

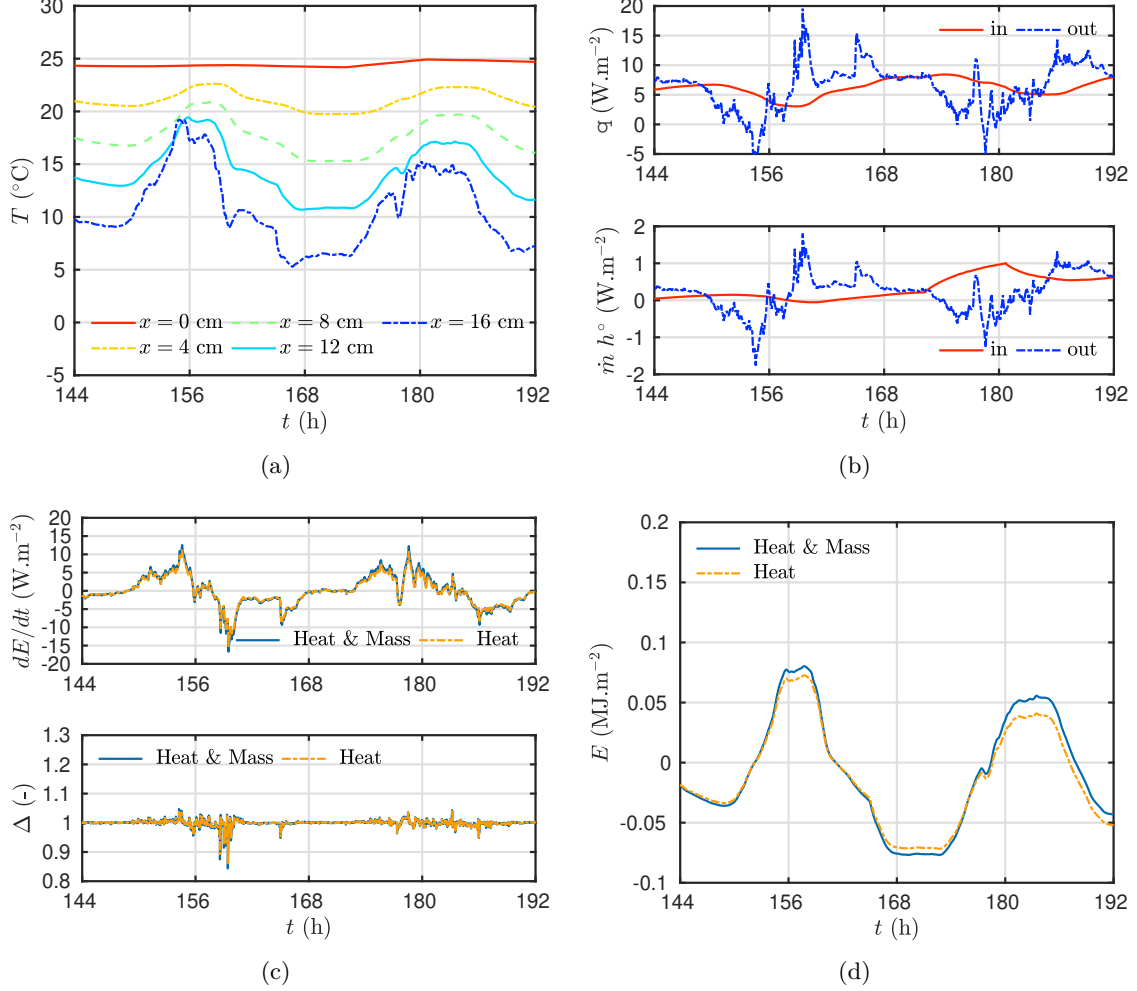


Figure 6. For the third period Ω_t^3 : time variation of computed temperature (a), heat flow rates (b), internal energy rate with Δ criteria (c) and cumulative internal energy (d).

These differences could of course be explained by the fact that the proposed metric considers better the inertial effect of the wall than the standard one. It is quite noticeable that values between the metric and the one proposed by [20] remains closed. But the exergy destruction rate presents also higher relative variations than for the lost work rate and less narrow variation. This means than values are closed because of the averaging integration when in dynamic state.

As remarked in Figures 7(a) and 7(b), the term $\left(1 - \frac{T_{\text{ext}}}{T_{\text{ins}}}\right) \cdot \mathbf{q}_{\text{in}}$ in Eq. (13) represents between 90% and 95% of the total work. This result may provide interesting outlooks. By monitoring accurately the heat flow rate on the inside part of the wall, together with the inside and exterior temperature, it is possible to assess the exergy loss of the wall. The above-mentioned hypothesis should be verified as the weather condition of the experiment do not represent various and vast climate configurations neither the variety of walls.

Finally, Tables 1 and 2 compare the proposed metric with the one from literature [20] presented in Section 2.5 for heat and coupled heat and mass transfer models, respectively. Due to the hypothesis on zeros fluctuation for energy and entropy, the metric (20) is only valid for long time interval. Results in the two tables present slight discrepancies between metrics from literature and the proposed one. The differences are explained by the hypothesis from STRUB's metric $\widetilde{W}_{\text{lost}}$. Differences increase when considering shorter periods of investigations. For instance, for day one, $\Phi_d = 19.89 \text{ kJ} \cdot \text{m}^{-2}$ and $\widetilde{W}_{\text{lost}} = 21.69 \text{ kJ} \cdot \text{m}^{-2}$ for period 1 with heat

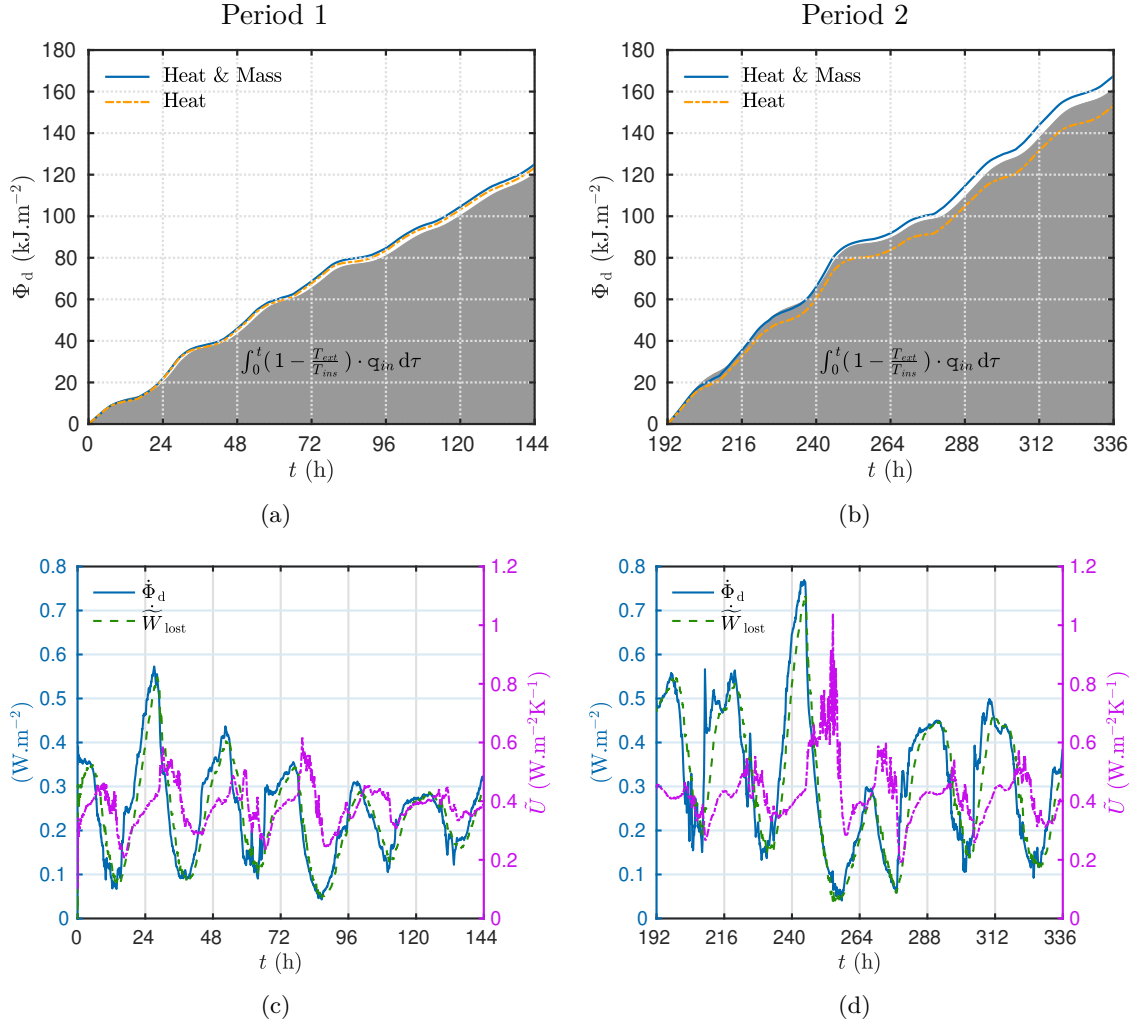


Figure 7. Time variation of the exergy loss and the lost work (a,b) and the exergy destruction rate and lost work rate (c,d) for first Ω_t^1 (a,c) and second Ω_t^2 (b,d) time period. The metric \tilde{U} is computed with coupled heat and mass transfer model.

transfer model, corresponding to a relative difference of 8%. If time period is decreased on a hourly period, a slight delay appears in time and amplitudes on variation are less important as mentioned for instantaneous values. The role of internal exergy variation being neglected, the intensity of irreversibilities and moments where they append is then out of view for analysing the behavior of the wall.

In addition, Tables 1 and 2 present the thermal load metric (19). It can be remarked that the rate of increase between the periods is lower than the lost available work metrics. The thermal load metric underestimates the load due to the increase of latent transfer during the second period, which raises the question of the relevance of this traditional metric. Last columns in Tables 1 and 2 gives the standard transmittance value evaluated in dynamic and steady state regime. The metric U has been computed considering standard values $h_{\text{ins}} = 8 \text{ W} \cdot \text{m}^{-2} \cdot \text{K}^{-1}$ and $h_{\text{ext}} = 12 \text{ W} \cdot \text{m}^{-2} \cdot \text{K}^{-1}$ for the surface transfer coefficients. The average value are quite close to the theoretical value, confirming that this coefficient will give good indications for the sizing of buildings. During the first period, where the latent heat transfer are negligible compared to sensible one, the dynamic and steady state based metrics provide similar results. However, such metric is not sensible to the increase of loss linked to the second period. The rate of increase (13.1%) is the lower of all metrics. The standard metric of transmittance U is then

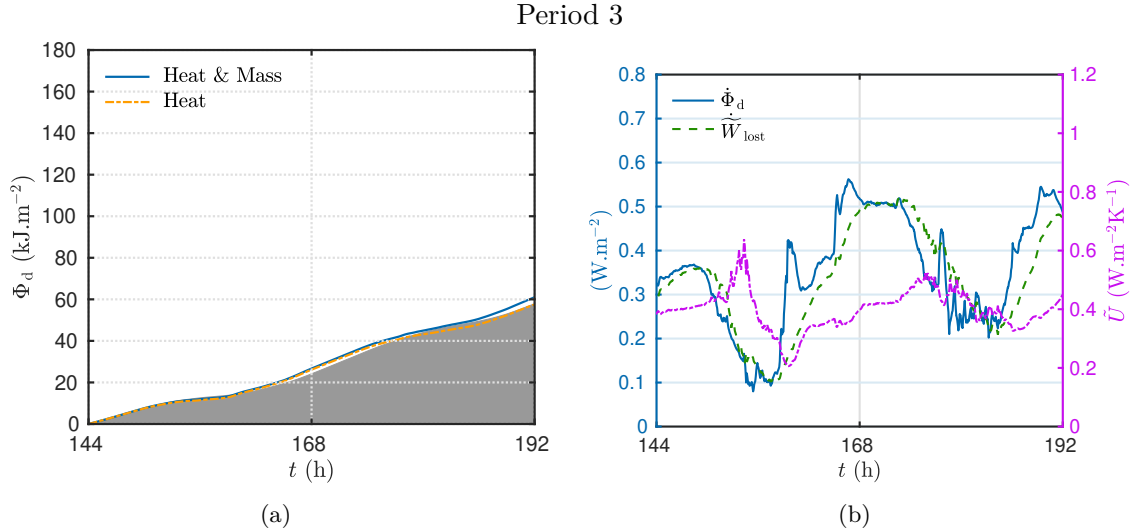


Figure 8. Time variation of the exergy loss and the lost work (a) and destruction exergy rate and the lost work rate (b) for third Ω_t^3 . The metric \tilde{U} is computed with coupled heat and mass transfer model.

not able to accurately evaluate the energy efficiency of the wall, due to its hypothesis based on steady state heat transfer only.

Table 1. Comparison of the metrics for assessing the wall energy efficiency, computed with only the heat transfer model.

Time period	Proposal		Literature		
	Φ_d [kJ.m ⁻²]	\tilde{W}_{lost} [kJ.m ⁻²]	Q [MJ.m ⁻²]	$\frac{1}{t_t} \int_{\Omega_t} \tilde{U} dt$ [W.K ⁻¹]	U [W.K ⁻¹]
Ω_t^1	123.4	119.3	2.6	0.38	0.4
Ω_t^2	153.2	148.11	2.9	0.39	0.4
Rate of increase [%]	24.1	24.1	10.7	2.6	—
Ω_t^3	57.6	55.2	1.0	0.38	0.4

4 Conclusion

Within the environmental context, the metrics to design energy efficient buildings are crucial. This article discuss several metrics to assess the energy efficiency of walls in transient dynamic conditions. The existing metrics are the thermal transmittance, the thermal loads and the lost available work defined in [20]. The proposed one is based on a thermodynamic analysis to evaluate the irreversibilities of the wall system. It requires the temperature field as well as inward/outward heat flow rates. They can be simply computed using a model based only on heat transfer, as performed in building designs, or using a coupled heat and mass transfer model. The discussion of the metrics is carried out for a real case study corresponding to a wall composed of wood fiber. Monitored data from an experimental demonstrator are used for the computations as boundary conditions.

The first step of the discussion was to verify the first principle of thermodynamic for both only

Table 2. Comparison of the metrics for assessing the wall energy efficiency, computed with the coupled heat and mass transfer model.

	<i>Proposal</i>		<i>Literature</i>		
	Φ_d	$\widetilde{W}_{\text{lost}}$	Q	$\frac{1}{t_f} \int_{\Omega_t} \widetilde{U} dt$	U
<i>Time period</i>	[kJ.m ⁻²]	[kJ.m ⁻²]	[MJ.m ⁻²]	[W.K ⁻¹]	[W.K ⁻¹]
Ω_t^1	125.0	120.4	2.6	0.38	0.4
Ω_t^2	167.6	161.3	3.1	0.43	0.4
<i>Rate of increase</i> [%]	34.0	33.9	19.8	13.1	–
Ω_t^3	61.0	57.8	1.01	0.4	0.4

heat and coupled heat and mass transfer models. It ensures that the computation of the fields (temperature, vapor pressure, heat flow rate) has been performed with a sufficient accuracy to evaluate further thermodynamic quantities, such as internal energy and entropy.

After this verification, the energy efficiency metrics are computed for three different periods. During the first one, the mass transfer through the wall is very small while during the second period, the latent effects scales with 10 % of the total heat flux. At least during the transient period, the metrics indicates how this transition is inefficient. Several conclusions can be highlighted from these investigations:

- (i) The proposed metric allows to assess the energy efficiency of the wall in dynamic and transient conditions. The exergy lost has a monotonous increase over time since it is related to the irreversibility of the system. The increase rate is lower when the wall is more efficient and, conversely, higher when the heat losses are important. Thus, periods of “good” or ”bad” efficiency of the wall can be detected with this metric.
- (ii) The assessment of (ii) is not possible with standard metrics as thermal conductance and thermal loads. The standard version of the thermal conductance completely underestimates the effect of time event and latent heat transfer. However it is very noticeable to see that measured values are closed to the theoretical value of design whatever the period. The thermal loads underestimates the influence of the latent effect in the energy losses and is not very sensitive to time event. The lost available work proposed in [20] is quite comparable offering lower value on considered period than the exergy destroyed. If, by definition, it only enables an evaluation over a whole time interval, the derivative use of this quantity gives a smoother value of the destruction exergy rate. That is why the integrate value are so similar. Nevertheless the approximation obtained by the quantity $\left(1 - \frac{T_{\text{ext}}}{T_{\text{ins}}}\right) \cdot \mathbf{q}_{\text{in}}$ offers interesting outlooks. With measurement of the inside and exterior temperature, combined with the inward heat flow rate, it could be possible to monitor the energy efficiency of the wall and detect faulty operations. However, it needs to verify the hypothesis for other wall configurations. In addition, it requires a precise measurement of the heat flux.
- (iii) the proposed metric is consistent with the increase of exergy destruction in transient period. This last point need to be evaluated with other transient regime such as temperature event.

Future works should also focus on extending the metric for multi-layer configurations and intermittent cooling/heating scenarios. In other words, this methodology is aimed to be used for consideration on other climate configurations, real arbitrary boundary conditions whatever the season is and for different multi-layer configurations.

Nomenclature and symbols

<i>Physical parameters</i>		
Latin letters		
A	area	$[\text{m}^2]$
c	heat capacity	$[\text{J} \cdot \text{kg}^{-1} \cdot \text{K}^{-1}]$
c_s	water specific heat capacity	$[\text{J} \cdot \text{kg}^{-1} \cdot \text{K}^{-1}]$
k	thermal conductivity	$[\text{W} \cdot \text{m}^{-1} \cdot \text{K}^{-1}]$
E, E	internal energy	$[\text{J}]$
ℓ	wall length	$[\text{m}]$
q, \mathbf{q}	heat flow rate	$[\text{W}]$
P_v	vapor pressure	$[\text{Pa}]$
Q	thermal transmittance	$[\text{J}]$
S, S	entropy	$[\text{K} \cdot \text{K}^{-1}]$
T, \mathcal{T}	temperature	$[\text{K}]$
t, t_f	time	$[\text{s}]$
U, \tilde{U}	thermal transmittance	$[\text{W} \cdot \text{K}^{-1}]$
\dot{W}	work rate	$[\text{W}]$
W, \tilde{W}	work	$[\text{J}]$
w	moisture content	$[\text{kg} \cdot \text{m}^{-3}]$
x	space coordinate	$[\text{m}]$
Greek letters		
Δ	first law error metric	$[-]$
δ	vapor permeability	$[\text{s}]$
Ω_t	time domain	$[\text{s}]$
Ω_x, Ω_x^i	space domain	$[\text{m}]$
ρ	density	$[\text{kg} \cdot \text{m}^{-3}]$
ϕ	relative humidity	$[-]$
$\dot{\Phi}$	exergy rate	$[\text{W}]$
Φ	exergy	$[\text{J}]$

<i>Subscript</i>	
<i>d</i>	destroyed
ins	inside ambient
in	inward to wall
irr	irreversibility
ext	exterior ambient
exc	exchange
f	final
out	outward the wall
lost	lost by the system
sys	system
Superscript	
0	reference state
^	measured quantity
Abbreviation	
HVAC	Heating, Ventilation, Air-conditioning

References

- [1] Energy statistics - an overview. https://ec.europa.eu/eurostat/statistics-explained/index.php?title=Energy_statistics_-_an_overview, 2020. 1
- [2] Energy performance of buildings directive. https://energy.ec.europa.eu/topics/energy-efficiency/energy-efficient-buildings/energy-performance-buildings-directive_en, 2021. 1
- [3] Journal Officiel de la République Française. Loi no 2015-992 du 17 août 2015 relative à la transition énergétique pour la croissance verte. <https://www.legifrance.gouv.fr/download/pdf?id=FMF1TotItrXlqeQwdI7cZ--nam6aCtsgM2LdqywZyGE=>, 2015. 1
- [4] Exigences réglementaires thermiques pour les bâtiments neufs. <https://www.ecologie.gouv.fr/exigences-reglementaires-thermiques-batiments-neufs>, 2020. 1
- [5] Réglementation environnementale RE2020. <https://www.ecologie.gouv.fr/reglementation-environnementale-re2020>, 2022. 1
- [6] ISO/TC 163/SC 2. ISO 6946:2017. Building components and building elements — Thermal resistance and thermal transmittance — Calculation methods, ISO, 2017. 2
- [7] Journal Officiel de la République Française. Décret relatif aux caractéristiques thermiques et aux exigences de performance énergétique des bâtiments nouveaux et des parties nouvelles de bâtiment, 2010-10-26. http://www.rt-batiment.fr/fileadmin/documents/RT2012/textes/Arrete_du_26_octobre_2010.pdf. 2
- [8] M. Mahmoodzadeh, V. Gretka, K. Hay, C. Steele, and P. Mukhopadhyaya. Determining overall heat transfer coefficient (U-Value) of wood-framed wall assemblies in Canada using external infrared thermography. *Building and Environment*, 199:107897, 2021. 2

- [9] T. Catalina, J. Virgone, and E. Blanco. Development and validation of regression models to predict monthly heating demand for residential buildings. *Energy and Buildings*, 40(10):1825–1832, 2008. [2](#)
- [10] M. J. Jiménez, B. Porcar, and M. R. Heras. Application of different dynamic analysis approaches to the estimation of the building component U value. *Building and Environment*, 44(2):361–367, 2009. [2](#)
- [11] F.P. Hollick, V. Gori, and C.A. Elwell. Thermal performance of occupied homes: A dynamic grey-box method accounting for solar gains. *Energy and Buildings*, 208:109669, 2020. [2](#)
- [12] A. Byrne, G. Byrne, A. Davies, and A. J. Robinson. Transient and quasi-steady thermal behaviour of a building envelope due to retrofitted cavity wall and ceiling insulation. *Energy and Buildings*, 61:356–365, 2013. [2](#), [6](#)
- [13] Y. Yang, Z. Chen, T. Vogt Wu, A. Sempey, and J.C. Batsale. In situ methodology for thermal performance evaluation of building wall: A review. *International Journal of Thermal Sciences*, 181:107687, 2022.
- [14] A. François, L. Ibos, V. Feuillet, and J. Meulemans. In situ measurement method for the quantification of the thermal transmittance of a non-homogeneous wall or a thermal bridge using an inverse technique and active infrared thermography. *Energy and Buildings*, 233:110633, 2021. [2](#)
- [15] S. Gasparin, J. Berger, D. Dutykh, and N. Mendes. An innovative method to determine optimum insulation thickness based on non-uniform adaptive moving grid. *Journal of the Brazilian Society of Mechanical Sciences and Engineering*, 41(4):173, 2019. [2](#), [7](#)
- [16] M. Kameni Nematchoua, P. Ricciardi, S. Reiter, and A. Yvon. A comparative study on optimum insulation thickness of walls and energy savings in equatorial and tropical climate. *International Journal of Sustainable Built Environment*, 6(1):170–182, 2017. [2](#)
- [17] M. Prek and V. Butala. Principles of exergy analysis of human heat and mass exchange with the indoor environment. *International Journal of Heat and Mass Transfer*, 53(25):5806–5814, 2010. [2](#)
- [18] C. E. K. Mady, M. S. Ferreira, J. I. Yanagihara, and S. de Oliveira. Human body exergy analysis and the assessment of thermal comfort conditions. *International Journal of Heat and Mass Transfer*, 77:577–584, 2014. [2](#)
- [19] M. Dovjak, M. Shukuya, and A. Krainer. Connective thinking on building envelope – Human body exergy analysis. *International Journal of Heat and Mass Transfer*, 90:1015–1025, 2015. [2](#)
- [20] F. Strub, J. Castaing-Lasvignottes, M. Strub, M. Pons, and F. Monchoux. Second law analysis of periodic heat conduction through a wall. *International Journal of Thermal Sciences*, 44(12):1154–1160, 2005. [2](#), [5](#), [6](#), [7](#), [12](#), [14](#), [15](#)
- [21] W. Choi, R. Ooka, and M. Shukuya. Unsteady-state exergy analysis for heat conduction of homogeneous solids under periodic boundary conditions. *International Journal of Heat and Mass Transfer*, 139:773–788, 2019. [2](#), [6](#)
- [22] W. Choi, R. Ooka, and M. Shukuya. Unsteady-state exergetic performance comparison of externally and internally insulated building envelopes. *International Journal of Heat and Mass Transfer*, 163:120414, 2020. [2](#)

- [23] W. Choi, R. Ooka, and M. Shukuya. Exergy analysis for unsteady-state heat conduction. *International Journal of Heat and Mass Transfer*, 116:1124–1142, 2018. [2](#), [6](#)
- [24] N. Mendes, M. Chhay, J. Berger, and D. Dutykh. *Numerical Methods for Diffusion Phenomena in Building Physics: A Practical Introduction*. Springer International Publishing, 2019. [3](#)
- [25] A. Jumabekova, J. Berger, A. Fouquier, and G.S. Dulikravich. Searching an optimal experiment observation sequence to estimate the thermal properties of a multilayer wall under real climate conditions. *International Journal of Heat and Mass Transfer*, 155:119810, 2020. [4](#)
- [26] J. Berger, D. Dutykh, N. Mendes, and B. Rysbaiuly. A new model for simulating heat, air and moisture transport in porous building materials. *International Journal of Heat and Mass Transfer*, 134:1041–1060, 2019. [4](#), [7](#)
- [27] S. Gasparin, J. Berger, D. Dutykh, and N. Mendes. An adaptive simulation of nonlinear heat and moisture transfer as a boundary value problem. *International Journal of Thermal Sciences*, 133:120–139, 2018. [5](#), [7](#), [8](#)
- [28] A. Bejan and A. Jones. *Advanced Engineering Thermodynamics*. Wiley Online, fourth edition, 2016. [5](#)
- [29] R. Pal. On the Gouy–Stodola theorem of thermodynamics for open systems. *International Journal of Mechanical Engineering Education*, 45(2):194–206, 2017. [6](#)
- [30] J.F. Sacadura. *Transferts thermiques*. Techniques et documentation edition, 1980. [6](#)
- [31] B. Tejedor, E. Barreira, R. M. S. F. Almeida, and M. Casals. Thermographic 2D U-value map for quantifying thermal bridges in building façades. *Energy and Buildings*, 224:110176, 2020. [6](#)
- [32] S. Rouchier, T. Busser, M. Pailha, A. Piot, and M. Woloszyn. Hygric characterization of wood fiber insulation under uncertainty with dynamic measurements and Markov Chain Monte-Carlo algorithm. *Building and Environment*, 114:129–139, 2017. [7](#)